RECRYSTALLIZATION CHARACTERISTICS OF TD-NICKEL

by

J. J. Petrovic, L. Leonard and L. J. Ebert

Prepared for

NATIONAL AERONAUTICS AND SPACE ADMINISTRATION
Grant NGR 36-003-094

Department of Metallurgy
CASE WESTERN RESERVE UNIVERSITY
Cleveland, Ohio

RECRYSTALLIZATION CHARACTERISTICS OF TD-NICKEL

NGR 36-003-094

ANNUAL STATUS REPORT

February 1969

Prepared by: J. J. Petrovic, L. Leonard and L. J. Ebert

Submitted to:

Office of Grants and Research Contracts
Attention: Code SC
National Aeronautics and Space Administration
Washington, D. C. 20546

Department of Metallurgy
CASE WESTERN RESERVE UNIVERSITY
Cleveland, Ohio

ABSTRACT

The portion of the total research program reported herein represents a determination of the characteristics and mechanism of recrystallization in TD-nickel, a model dispersion hardened system. Recrystallization behavior after rolling and swaging deformations was examined in two forms of TD-nickel, as-extruded and commercial one inch bar. Efforts to date have centered on an investigation of deformation and annealing substructures by transmission electron microscopy.

Recrystallization in TD-nickel is observed to be highly dependent upon character of prior deformation, with some deformation types producing recrystallization resistance. The outstanding substructural difference between recrystallization-resistant and recrystallization-prone deformations is that the former preserves the initial grain boundary structure, while the latter appears to severely alter it.

Recrystallization-resistant structures exhibit recovery after annealing at recrystallization temperatures. Recrystallization significantly lowers the dislocation density. No evidences were found of extensive dislocation-thoria particle networks within the recrystallized substructure, although isolated small regions of recovery were observed.

All ambient temperature deformations examined in the present study produced voids at a significant fraction of thoria particles. Voids appeared to "heal" after annealing at elevated temperatures. The degree of void formation was similar after both recrystallization-resistant and recrystallization-prone deformations, indicating that this phenomena does not control recrystallization in TD-nickel.

TABLE OF CONTENTS

LIST OF TABLES

LIST OF FIGURES

LIST OF FIGURES CON'T

INTRODUCTION

TD-nickel is a two-phase alloy, containing approximately 2 volume percent thoria (ThO_2) particles as a fine, inert dispersion in a nickel matrix. The dispersion is produced by powder metallurgy techniques, with the introduction of mechanical working beyond that required for compaction. This fabrication procedure (the details of which are proprietary) results in a substructure which is extremely stable at elevated temperatures. Due to this stability, TD-nickel is a significant base material for elevated temperature applications.

Recently, it has been shown that the ambient and elevated temperature mechanical properties of TD-nickel are controlled by different mechanisms (1)*. During room temperature testing, these properties exhibit typical response to mechanical working and annealing operations, with intra-granular substructure the influencing factor. However, at elevated temperatures strength levels appear to be controlled by grain boundary considerations. Fracture occurs at low strains by intergranular separation in regions where the applied load is normal to the grain boundary surface area. It is thus proposed that a preponderance of grain boundaries aligned parallel to the applied stress (or a scarcity of grain boundaries) is a necessary condition for elevated temperature strengthening in this dispersion hardened alloy.

Since grain boundary considerations play a significant role in determining the mechanical properties of TD-nickel at anticipated use temperatures, a process such as recrystallization which, in this material, drastically alters the amount of grain boundary surface area and boundary orientation, can be expected to affect mechanical properties also. In fact, it has been observed that the recrystallization process does not degrade, but rather enhances high temperature strength (1).

In the light of the above, it is important to obtain a basic

---

*Numbers in parentheses refer to Bibliogrphy at the end of the report.

understanding of the recrystallization process in TD-nickel, because such an investigation may lead to an optimization of the properties of this commercially interesting material. Also, since TD-nickel is a model example of a dispersion hardened system, the results of a recrystallization study may lend insight into the operation of this phenomena in other dispersion hardened alloys. This, then, is the intent of the present investigation.

The present report is a summary presentation of the research completed during the period January 1968 to January 1969. This research has taken the form of an electron microscopy investigation designed to characterize the substructures of: 1) as-received TD-nickel in two commercial forms; 2) rolling and swaging deformation substructures; 3) annealing and recrystallization substructures.

MATERIAL

TD-nickel supplied by the E. I. duPont de Nemours Company (new supplier of TD-nickel is Fansteel) was used in the present investigation. The alloy is made by the chemical production of a thoria containing nickel powder, the compaction and sintering of the powder into a billet, and final densification by warm extrusion. The extruded product is subsequently processed into commercially useable bar, wire, tubing or sheet.

Two forms of TD-nickel, as-extruded and commercial one inch bar, were used in the present study. Both originated from the same sintered billet. The first form, though not suitable for commercial application, represents a state of minimum mechanical working of the material. The second is a commercially useable end product. Chemical composition of the particular lot of material used is given in Table 1.

The microstructure of the as-extruded material consists of grains approximately 2 microns by 4 microns in size, elongated in the extrusion direction. In the commercial one inch bar, grain elongation parallel to the bar axis is much more extreme, with grain dimensions of 1 micron by 15 microns. The commercial bar possesses a very strong duplex fiber texture of <200> and <111> components (1). This texture is also present in the as-extruded material, but is much weaker. Neither form of TD-nickel will recrystallize after one hour at 2400^{o}F (1).

BACKGROUND FOR THE PRESENT INVESTIGATION

The recrystallization behavior of TD-nickel has received relatively little attention in the past (1-7). It is generally acknowledged that the presence of the thoria dispersion makes recrystallization more difficult as compared to pure nickel; in TD-nickel the recrystallization process requires higher temperatures than in pure nickel.

However, a highly unusual aspect of TD-nickel recrystallization has recently come to light (1). It has been shown that the recrystallization process is quite sensitive to type of prior deformation. Tables 2 and 3 illustrate this behavior for as-extruded and commercial one inch bar materials from the same lot of TD-nickel used in the present investigation. Figures 1 and 2 indicate the types of rolling passes used. These data have served as a basis for the present study.

Data in Table 2 indicate that swaging deformations completely inhibit the recrystallization process. The influence of rolling direction on recrystallization is most marked in the commercial bar, where recrystallization occurs readily with transverse rolling, but is totally suppressed by longitudinal rolling. This difference correlated with a difference in deformation texture (1). Transverse rolling produced a cube texture, while longitudinal rolling caused a copper texture. Sharpening of the initial duplex fiber texture occurred with swaging.

This influence of deformation character on the recrystallization process has not received explicit mention in previous investigations of TD-nickel, possibly because of the limited efforts in this area. However, where commercial bar and rolling deformations have been used (2,7), the prior deformation producing recrystallization always involved the application of some degree of transverse rolling.

When TD-nickel is deformed in a suitable manner to cause recrystallization to occur readily, the phenomena proceeds over a

relatively narrow temperature range, as is shown in Table 3 for transverse rolling deformations. Microstructurally, an unusually large recrystallized grain size is produced, with the grains being millimeters in size, and thus quite visible to the naked eye.

Thus far, the present investigation has concerned itself with a transmission electron microscopy examination of the substructures produced by the various deformation processes shown in Tables 2 and 3, and the substructures derived from these on subsequent annealing. The approach has been to provide a general characterization of each substructure, in the hopes that differences in substructure will correlate with the observed differences in recrystallization behavior and shed some light on the basic mechanisms of this phenomena in TD-nickel. Of particular interest were differences in dislocation configurations and grain boundary arrangements.

EXPERIMENTAL PROCEDURE

The deformed materials studied were remnants of the specimens used to derive the data in Tables 2 and 3. This material was used to optimize correlation with previous work in the contractual program. All annealing was performed in air, with the temperature controlled to $\pm$ 5°F. The maximum annealing temperature employed was 2300°F. Since the thoria particle distribution has been shown to be stable up to a temperature of 2450°F (8), it is probable that no particle coarsening occurred during any of the heat treatments.

To obtain transmission electron microscopy specimens from the bulk material, flat sheets approximately 0.020" in thickness were machined from the bulk. Discs 1/8" in diameter were then spark cut from the sheet by a trepanning operation. Considerable care was taken to insure that spark cutting in no way altered the initial specimen structures.

The dimple technique was employed to produce thin foils of TD-nickel. This involved two operations. First, starting with a 1/8" diameter 0.020" thick disc, indentations (i.e. "dimples") approximately 0.003" deep and 1/16" in diameter were introduced on opposite sides of the disc near the center of its diameter. This was accomplished by jet machining with a solution of 35% H_2SO_4, 40% H_3PO_4, 25% H_2O at 5 volts and 100 milliamperes. The disc specimen was seated in a teflon holder, with a platinum wire contact. A 1/16" diameter syringe cathode with gravity feed of the polishing solution was the jet machining tool. With this arrangement, a removal rate of approximately 0.001" per minute was observed.

The dimpled specimen was then removed from the teflon holder and immersed in the 35% H_2SO_4, 40% H_3PO_4, 25% H_2O solution, using platinum tipped tweezers as the electrical contact and platinum wire as the cathode. It was necessary to use platinum because of the highly corrosive nature of the polishing solution. Polishing was then continued at 5.5 volts and approximately 200 milliamperes until a small perforation was observed at the center of the disc. This

perforation was detected by illuminating the backside of the disc with a high intensity light source and observing a magnified image of the front of the disc for the first pinpoint of transmitted light, whereupon polishing was discontinued as quickly as possible. The specimen was rinsed, in consecutive order, with the following: 1) fresh polishing solution (to remove loose thoria particles); (2) distilled water; 3) methyl alcohol; 4) ethyl alcohol; 5) ether.

The technique just described produced excellent transmission electron microscopy specimens. Although other polishing solutions were investigated, the 35% H_2SO_4, 40% H_3PO_4, 25% H_2O solution was by far the best for TD-nickel, producing a brilliant polish. At perforation of the specimen, the rim of the disc was approximately 0.003" thick. Hence, the removal of any damaged layer due to machining or spark cutting was assured. Also, the thin nature of the finished specimen aided resolution in the electron microscope, as nickel is ferromagnetic.

A JEM-6A electron microscope operated at 100 kv (camera constant 2.33 Å-cm) was used for viewing specimens. Since a substructural characterization was desired, the following procedure was adopted to study each specimen. First, a number of low magnification micrographs (10,000X) were obtained as a general foil survey. Then, the magnification was raised to 20,000X and representative substructural features analyzed through a sequence of micrographs of each area. This sequence was: 1) 20,000X micrograph of a region of interest; 2) superposition of the 20,000X area micrograph and the position of the selected area diffraction blades; 3) selected area diffraction pattern; 4) 20,000X micrograph of the same region after tilting (usually about 1^{o}).

The above procedure was found to reveal a maximum amount of information about a given foil area using a minimum number of micrographs. The superimposed SAD blade-area micrograph determined the exact area from which the subsequent diffraction pattern was being obtained. Tilting of the specimen made it possible to distinguish foil features such as dislocations and boundaries from extraneous features such as extinction bend contours.

RESULTS AND DISCUSSION

The various materials, deformation states, annealing conditions, and specimen orientations examined thus far in the present study are listed in Table 4.

Much attention was focused on determining the substructures of the as-received extruded and commercial bar materials, since these formed the basis for further comparisons. Representative micrographs of these materials are shown in Figures 3 and 4. In the as-extruded material, Figures 3a and 3b, the grains appear nearly equiaxed with sizes in the range of 2-4 microns as previously reported (1). Most of the grain boundaries are high angle in nature (i.e. a misorientation of more than about 5^{o}). However, low angle boundaries with misorientations less than 5^{o} were observed within some grains. A range of orientations was seen, the most common being <110>, <310>, <001>, and <211>. In foils oriented parallel to the extrusion axis, a <001> grain orientation was predominant, in agreement with the observed <001> - <111> duplex fiber texture in this material. The dislocation density seemed relatively high and some dislocation arrays were observed.

The commercial bar grain structure consisted of grains elongated along the bar axis, Figures 4a - 4d. The observed grain dimensions, again in agreement with previous studies, were 1 micron by about 15 microns. Trace analysis showed the crystallographic grain elongation direction to be <001>, in agreement with the literature (2). This being the case, in foils oriented parallel to the bar axis, virtually all grains examined possessed <001> foil normals. Rather surprisingly, no clear manifestation was found of the <111> component of the commercial bar fiber texture. However, the <100> component was quite prominent. As with the as-extruded material, most of the grain boundaries observed were high angle, with adjacent grains being related by rotations about their <100> elongation directions. In foils oriented perpendicular to the bar axis, very little rotation was evident between adjacent grains. In this material also, some small angle boundaries were observed. The dislocation

density in the commercial bar was similar to that in the as-extruded material.

Dislocation configurations in both commercial bar and as-extruded materials usually took the form of a cell structure, with most dislocations pinned by thoria particles. The fact that some regular dislocation arrays and small angle boundaries were observed in these materials may be indicative of stress relieving in fabrication.

Micrographs of recrystallization-resistant deformation substructures for both as-extruded material and commercial bar TD-nickel are displayed in Figures 5-8. Deformation substructures more prone to recrystallization are shown in Figures 9-11. Comparison of these micrographs reveals that recrystallization-resistant substructures are characterized by well defined grain boundaries, unlike recrystallization-prone substructures.

For more detailed comparison of microstructural differences, it is worthwhile to restrict discussion to the commercial bar material only, because this substructure is initially more uniform than that of the as-extruded state. Also, deviations in recrystallization behavior are most marked in the commercial bar.

Figures 12 and 13 consist of higher magnification micrographs representative of the deformation substructures giving extremes in recrystallization behavior in the commercial bar. The micrographs are accompanied by selected area diffraction patterns (correctly oriented to compensate for lens rotation in the electron microscope). Changes in the substructures on tilting of the specimens are also indicated.

The recrystallization-resistant deformation structure of Figure 12 shows many high angle boundaries, presumably elongated in the rolling direction. A well developed dislocation cell structure is evident within the individual grains. The selected area diffraction pattern, with much streaking of diffraction spots, is representative of a highly deformed structure. This diffraction pattern, taken of many grains, indicates a high degree of texturing, with adjacent grains apparently misoriented by rotations about the foil normal (which in this case is parallel to the rolling plane normal). The

diffraction pattern itself is basically <110>, which is close to the <123>, <146> rolling plane normal observed for this deformation structure in macroscopic x-ray pole figures (1).

The recrystallization-prone deformation structure of Figure 13 differs from that previously discussed in that very few sharp, high angle boundaries are visible. The dislocation density is high, but a well defined cell structure does not appear to be present. The selected area diffraction pattern, from an area which in the undeformed state would contain a number of highly misoriented grains, is an unusually uniform <001> (in agreement with the macroscopic pole figure). Streaking of the spots again indicates a deformed structure.

The apparent disappearance of high angle boundaries with recrystallization-prone deformation is very difficult to rationalize. It is possible that recrystallization has occurred in the thin foil in the microscope; however, this is highly unlikely because of the high dislocation density observed. Also, recrystallization in foils of pure nickel could only be produced by electron beam heating with the removal of the condensor aperture (which was never done in the present investigation)(9).

At the present time, it is not yet certain whether the recrystallization tendency dependence on cell structure is a true effect, nor is a suitable mechanism obvious should it be. However, were this actually the case, it might explain the large recrystallized grain size and narrow temperature region for recrystallization in TD-nickel, if one postulates a mechanism of subgrain formation and subsequent growth within a large (essentially single crystal) volume of high dislocation density produced by deformation. The rate of development of this type of microstructure with degree of deformation is indicated by comparing Figures 14 and 15.

Substructural changes resulting from annealing in a specimen deformed so as to exhibit recrystallization-resistance are indicated in Figure 16. The high angle grain boundaries have become quite distinct. Grains possess nearly the same orientations as they had in the deformed state. Spots in selected area diffraction patterns have

sharpened considerably (as compared to those observed after deformation and prior to annealing), suggesting that the crystal lattice is no longer severely distorted. The dislocation density appears substantially reduced. The occurrence of low angle boundaries is high. On the whole, the substructure indicates a recovered material, not dissimilar to the initial states of the as-extruded and commercial bar materials.

The character of the recrystallized condition in TD-nickel has been studied to some degree in order to clarify certain observations in the literature. TD-nickel exhibits "true" recrystallization behavior in that recrystallization appreciably lowers the dislocation density from that of the deformed state. In Figure 17, diffraction conditions were such as to optimize contrast from dislocations. The dislocation density is low. In the present investigation, no evidences were found of a residual dislocation-thoria particle network within recrystallized grains, as reported by some workers (6). However, a number of very fine extinction bend contours seemingly associated with the thoria particles were observed. Without some care, these might be mistaken for dislocations.

The recrystallized structure contains a high density of fine twins. In addition, a small-scale, unrecrystallized remnant structure, as shown in Figure 18, is present. Very few such areas were observed in the thin foils examined. However, because of the small field of view in the electron microscope, the fact that they were observed at all indicates that, from a macroscopic viewpoint, these areas may comprise a small, but significant, portion of the "recrystallized" state. The regions themselves appear to possess a recovered substructure, containing low angle boundaries and a dislocation density higher than that of the surrounding recrystallized areas. Such regions may account for the x-ray observations of Grierson and Bonis, who note the presence of elastic strains in recrystallized TD-nickel (4).

During the course of the examination of deformation substructures, it was noted that large-scale room temperature deformations seemingly produce voids at thoria particles (i.e., a decohesion of particle and surrounding matrix). A typical example may be seen in

Figure 19. This void formation was extensive and occurred in all deformation substructures observed. The voids appear elongated in the direction of deformation. This phenomena was not the result of thin foil preparation, because no voids could be seen in the initial as-extruded or commercial bar substructures. The voids apparently were "healed" by high temperature annealing, for very few were observed in annealed or recrystallized materials. Presence of the voids corroborates the observation of this phenomena by other workers (5,10). However, the contention by Webster (5) that such voids control recrystallization behavior in TD-nickel systems has not received support from the present investigation. Void densities were approximately the same after both recrystallization-resistant and recrystallization-prone deformations, which indicates that the presence of thoria particle voids cannot be a major influence on the TD-nickel recrystallization process.

FUTURE WORK

At the present time, analysis of the deformation and annealing substructures of TD-nickel by transmission electron microscopy is nearly complete. Some work remains in determining a more complete three-dimensional representation of key deformation structures and certain annealing substructures must yet be examined.

In a recrystallization study of TD-nickel, the ideal approach might be to examine incipient nucleation of recrystallized grains by transmission electron microscopy, in order to establish the recrystallization mechanism. Although this has been attempted, preliminary results have been negative since a suitable combination of annealing temperature and time has not been discovered. Indeed, no such study is present in the literature, which may indicate that the kinetics of recrystallization in TD-nickel preclude such an approach. In any case, an investigation of the exact temperature-time dependencies of recrystallization in the as-extruded and commercial bar materials will be undertaken in the hopes of examining the recrystallization process directly. Attempts may also be made to induce recrystallization in the electron microscope by electron beam heating, should other methods fail.

Indirect techniques shedding light on the recrystallization process will be employed. In pure nickel, workers have observed two recrystallization mechanisms to be operative. At low deformations, the migration of high angle grain boundaries already present in the deformed structure is a reported recrystallization mechanism (11). Coalescence of subgrains and the subsequent growth of new recrystallized grains is the indicated process at high deformations (9,12). Since TD-nickel might be expected to exhibit one of these two mechanisms, data supporting one or the other process may be derived from a recrystallized pole figure. The grain migration mechanism is indicated if the recrystallized pole figure is similar to the corresponding deformation pole figure, while a dissimilar comparison supports the formation of new recrystallized grains. Because of the large recrystallized

grain size of TD-nickel, conventional pole figure methods cannot be employed. Instead, the pole figure will be determined by analysis of Laue back reflection x-ray diffraction patterns from individual recrystallized grains.

Another indirect means for investigating the recrystallization process is a comparison of recrystallization activation energies of as-extruded and commercial bar materials (assuming the process in TD-nickel follows Arrhenius-type kinetics) with that of pure nickel. Further, a recrystallized grain size comparison of as-extruded and commercial bar as a function of annealing temperature and time may be informative. This latter study must be qualitative in nature, since the large recrystallized grain size precludes a proper statistical investigation.

Of special significance is the planned examination of the recrystallization behavior of once recrystallized TD-nickel. Material will be recrystallized, then deformed and recrystallized a second time. Investigation of the second recrystallization process allows the examination of the inherent behavior of the dispersion, without complication from other structural features such as grain boundaries and texturing. Should second recrystallization prove different from the primary recrystallization process, this would indicate that recrystallization in TD-nickel is controlled to some degree by its fabricated structure, as well as by the presence of the oxide particle dispersion.

Practically, such a study also has merit since it may yield a technique for producing a fine recrystallized grain size in commercially useable TD-nickel products. For elevated temperature applications, such a microstructure may be desirable in view of the sensitivity of high temperature mechanical properties to grain boundary factors.

REFERENCES

1. G. S. Doble, L. Leonard and L. J. Ebert, NASA Research and Development Report NGR 36-003-094, Final Report, November 1967.

2. M. C. Inman, K. M. Zwilsky and D. H. Boone, Trans. ASM, 57, (1964) 701.

3. M. von Heimendahl and G. Thomas, Trans. AIME, 230, (1964),1520.

4. R. Grierson and L. J. Bonis, Trans. AIME, 239, (1967), 622.

5. D. Webster, Trans. AIME, 242, (1968), 640.

6. A. Bassi, G. Camona, M. Conserva and P. Fiorini, Memoires Scientifiques Rev. Metallurg., LXIV, no. 6, (1967), 547.

7. B. A. Wilcox and R. I. Jaffee, Trans. JIM, 9, (1968), Supplement, 575.

8. M. C. Inman and P. J. Smith, Oxide Dispersion Strengthening (1966).

9. L. C. Michels and B. G. Ricketts, Trans. AIME, 239, (1967), 1841.

10. G. S. Ansell, private communication.

11. J. E. Bailey and P. B. Hirsch, Proc. Roy. Soc., 267A, (1962),11.

12. W. Bollmann, J. Inst. Met., 87, (1959), 439.

TABLE 1

VENDORS CHEMICAL ANALYSIS OF TD-NICKEL LOT 2294

Element	Weight %
C	0.0038
Ti	0.001
Fe	0.002
Cr	0.001
Co	0.01
Cu	0.003
S	0.002
ThO_2	2.4

TABLE 2

RECRYSTALLIZATION IN AS-EXTRUDED TD-NICKEL
AFTER ONE HOUR HEAT TREATMENTS

Rolling Reduction (%)	% Recrystallized 2400°F	2300°F	2000°F
		LONGITUDINAL PASS	
21	91	95	0
37	97	99	30
59	99	99	11
74	97(0)(80)	100(0)(80)	16
85	100(0)(50)	100(0)(50)	50(0)(10)
90	0	0	0
		TRANSVERSE PASS	
20	100	85	0
36	98	65	1
59	95	90	5
74	95	95	25
85	100(50)*(80)**	80(0)(60)	2
88	100(0)(80)	100(0)(60)	0

Swaging Reduction (%)	2400°F
14	0
26	0
59	0
75	0
82	0
90	0
95	0

* = % Recrystallized at Surface

** = % Recrystallized Overall

TABLE 3

RECRYSTALLIZATION IN COMMERCIAL TD-NICKEL ONE INCH BAR AFTER ONE HOUR HEAT TREATMENTS

Rolling Reduction (%)	2400°F	2300°F	2000°F	1500°F	1250°F	1000°F
			LONGITUDINAL PASS			
21	0					
37	0					
59	0					
74	0					
82	0					
87	0					
			TRANSVERSE PASS			
22		0	0	0	0	0
37		99	97	25	2	0
59		100	100	80	52	5
74		100	100	95	95	0
83		100	100	100	100	0
87		100	100	100	100	0

Swaging Reduction (%)	2400°F
14	0
26	0
45	0
59	0
75	0
82	0
90	0
95	0

TABLE 4

MATERIAL STATES EXAMINED IN THE PRESENT INVESTIGATION

Material	Deformation Condition and Degree	Annealing Temp. (°F)*	Orientation**
As-extruded	None	none	Perpendicular
As-extruded	none	none	Parallel
Commercial Bar	none	none	Perpendicular
Commercial Bar	none	none	Parallel
As-extruded	Longitudinal rolling 59%	none	Perpendicular
As-extruded	Longitudinal rolling 90%	none	Perpendicular
As-extruded	Transverse rolling 88%	none	Perpendicular
As-extruded	Swaged 90%	none	Parallel
As-extruded	Swaged 90%	none	Perpendicular
Commercial Bar	Longitudinal rolling 87%	none	Perpendicular
Commercial Bar	Transverse rolling 22%	none	Perpendicular
Commercial Bar	Transverse rolling 37%	none	Perpendicular
Commercial Bar	Transverse rolling 83%	none	Perpendicular
Commercial Bar	Swaged 90%	none	Parallel
Commercial Bar	Swaged 90%	none	Perpendicular
Commercial Bar	Longitudinal rolling 87%	2300	Perpendicular
Commercial Bar	Transverse rolling 87%	2300	Perpendicular

* All Annealing for one hour

** Foil normal either parallel or perpendicular to final working direction.

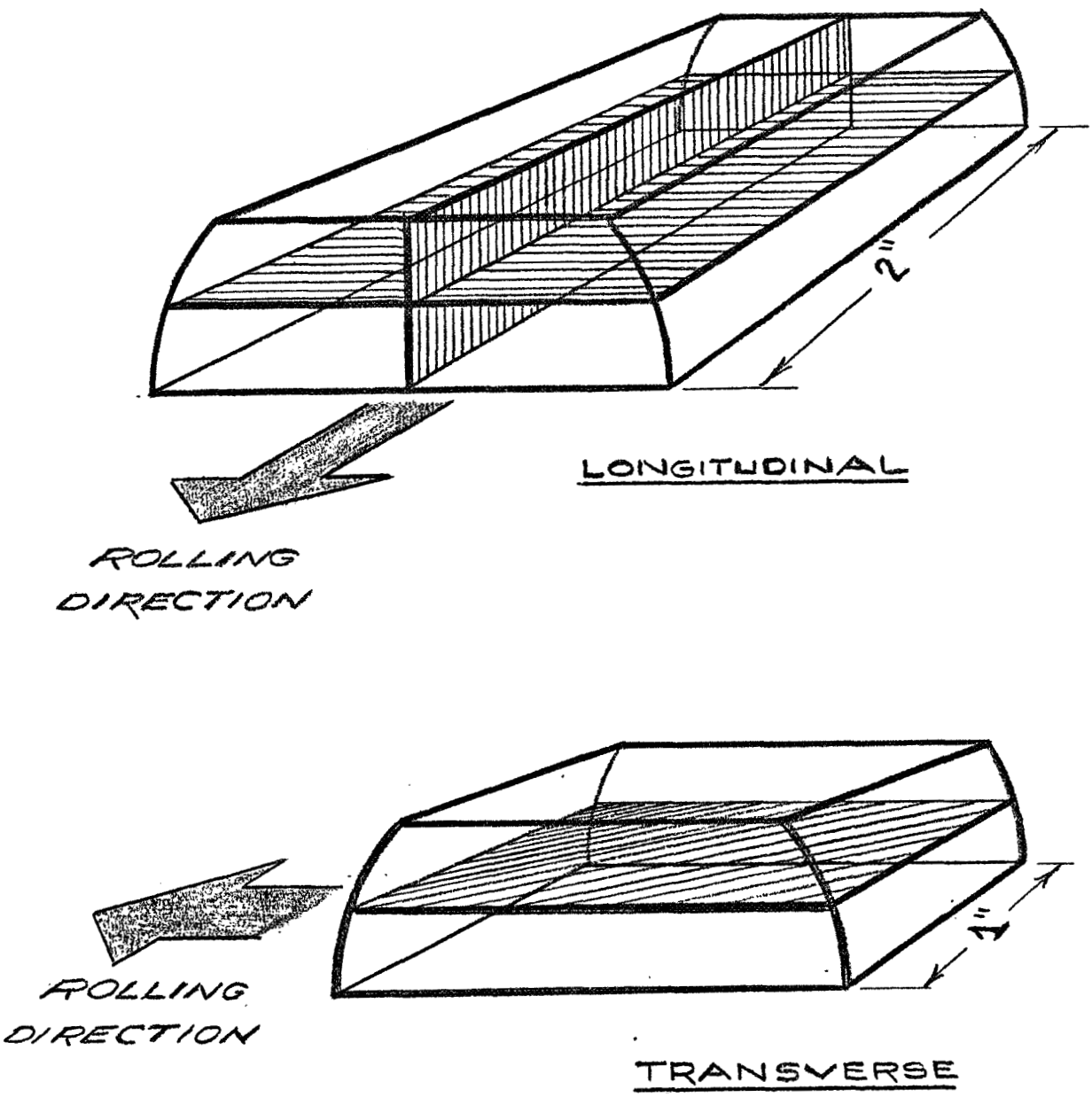

Figure 1. Sectioned pieces and rolling directions of as-extruded TD-nickel (initial thickness $\frac{1}{4}$").

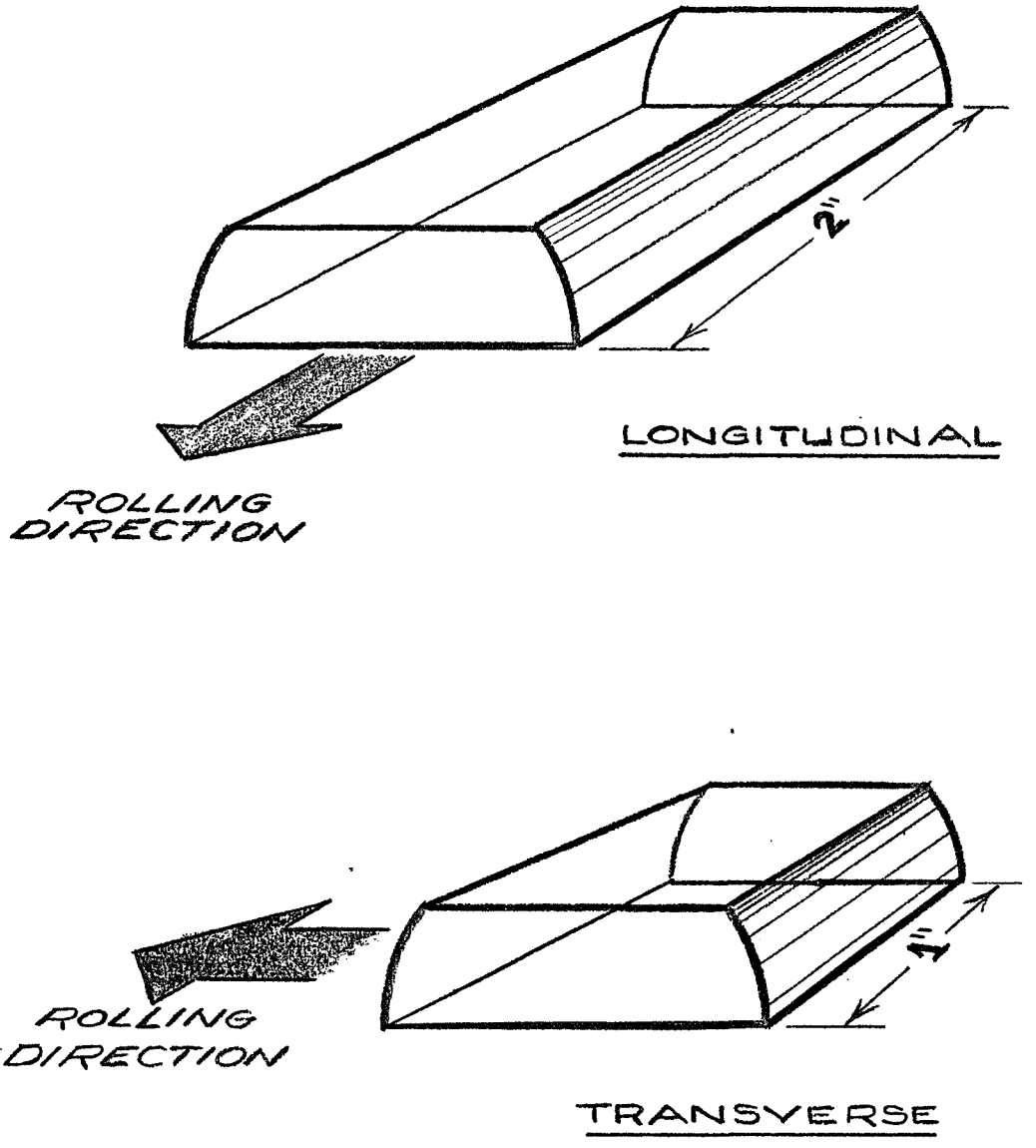

Figure 2. Sectioned pieces and rolling directions of commercial one inch bar TD-nickel (initial thickness $\frac{1}{4}$")

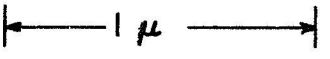

a) Foil normal perpendicular to extrusion axis. Note dislocations at A, probable low angle boundary at B, high angle boundary at C.

Figure 3. As-extruded TD-nickel.

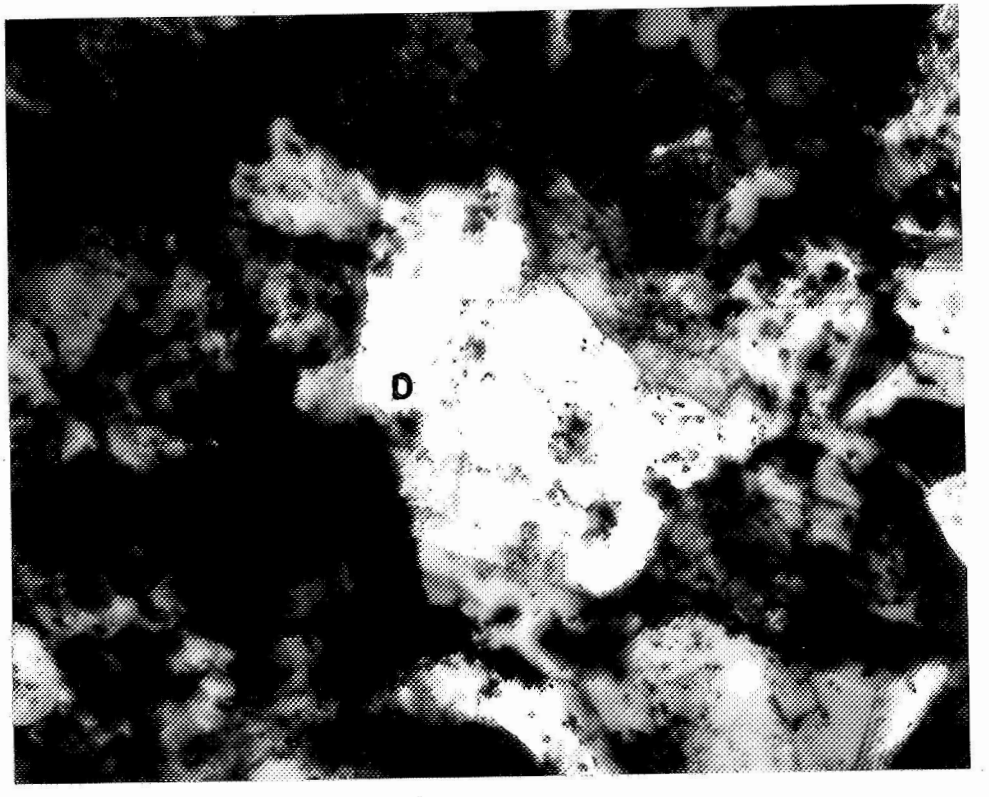

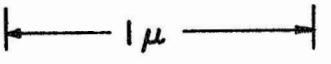

b) Foil normal parallel to extrusion axis. Note dislocation array at D.

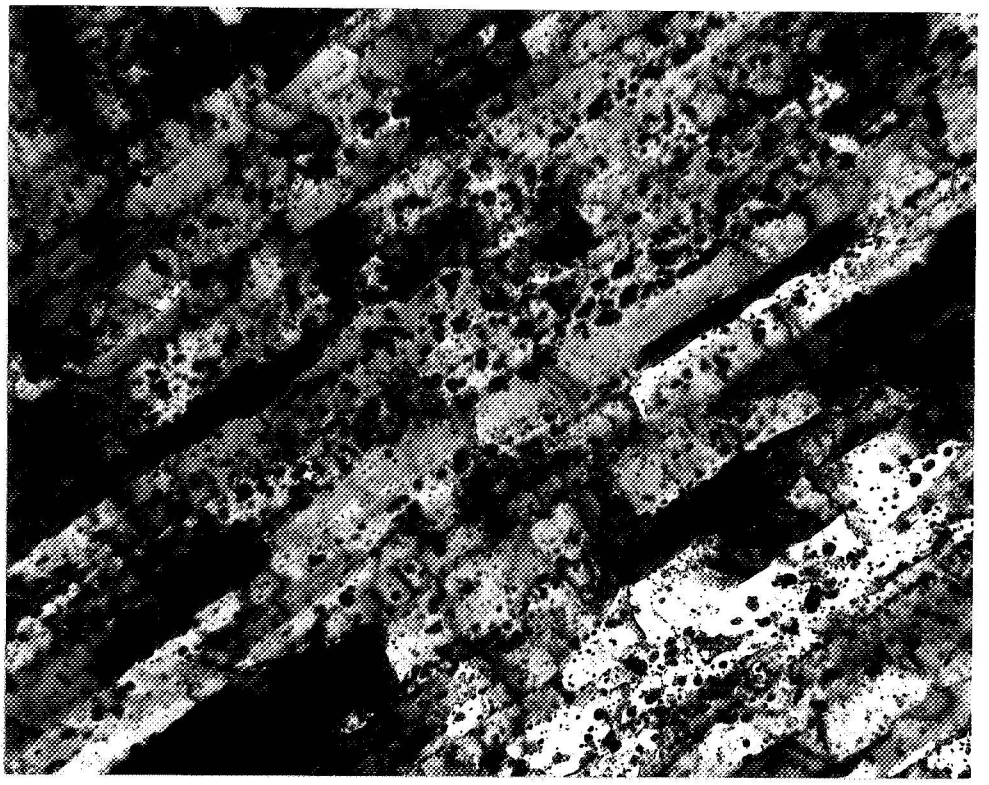

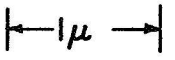

a) Foil normal perpendicular to bar axis (low magnification).

Figure 4. Commercial one inch bar TD-nickel.

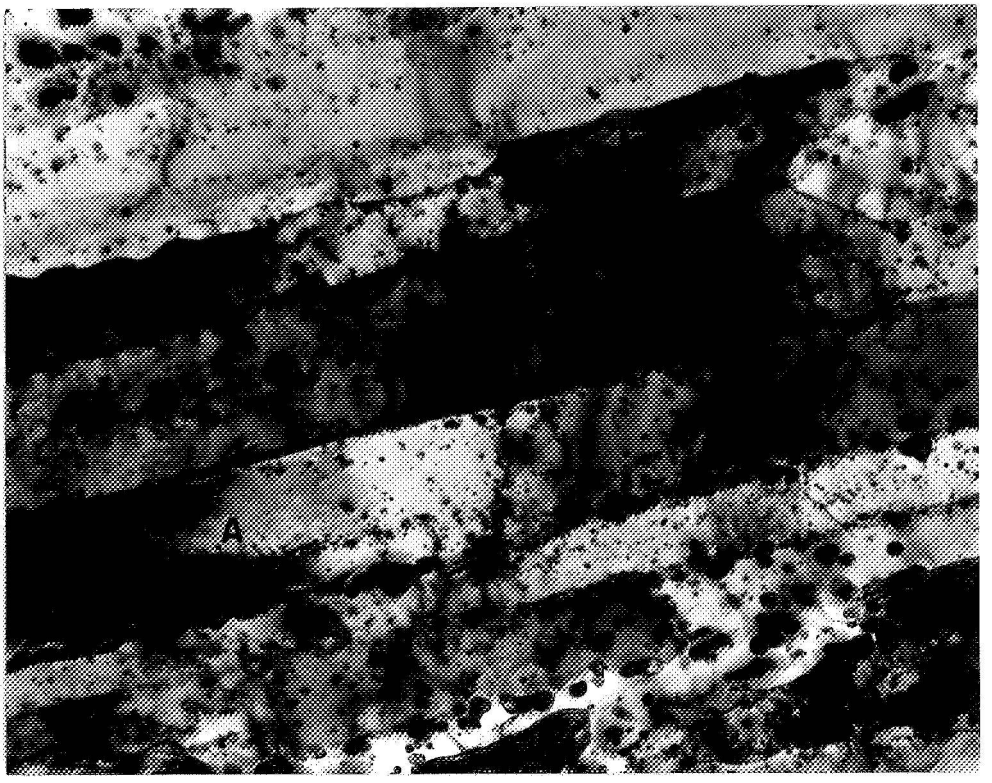

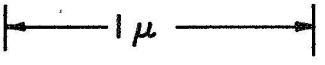

b) Foil normal perpendicular to bar axis (high magnification). Note probable low angle boundary at A.

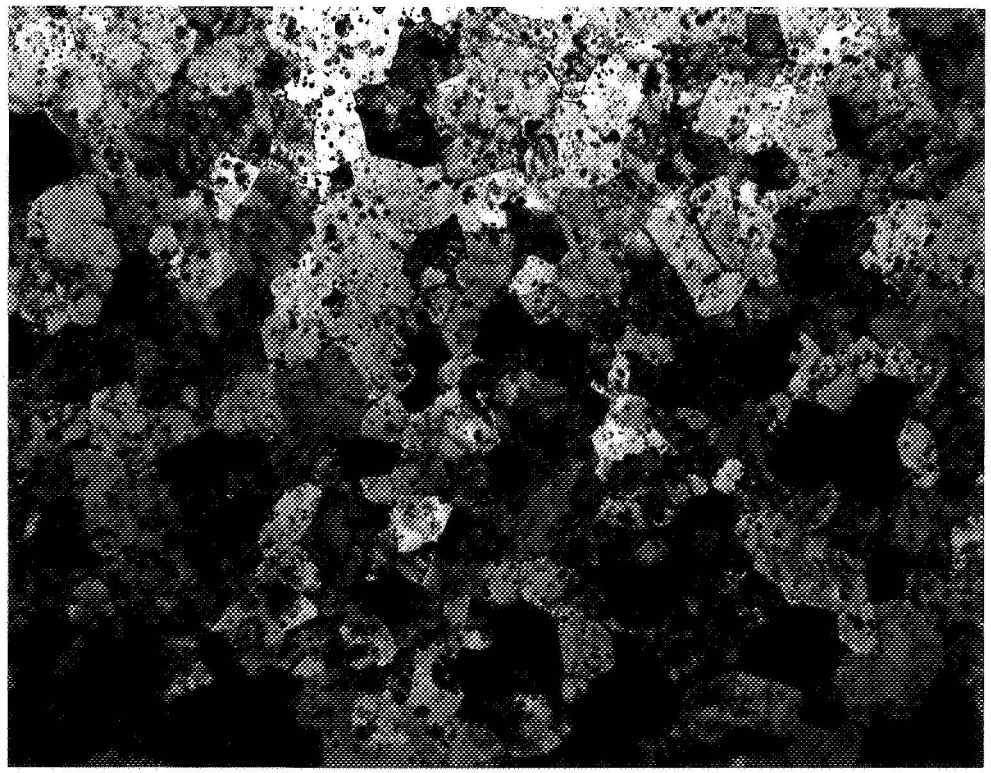

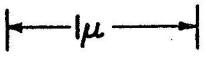

c) Foil normal parallel to bar axis (low magnification).

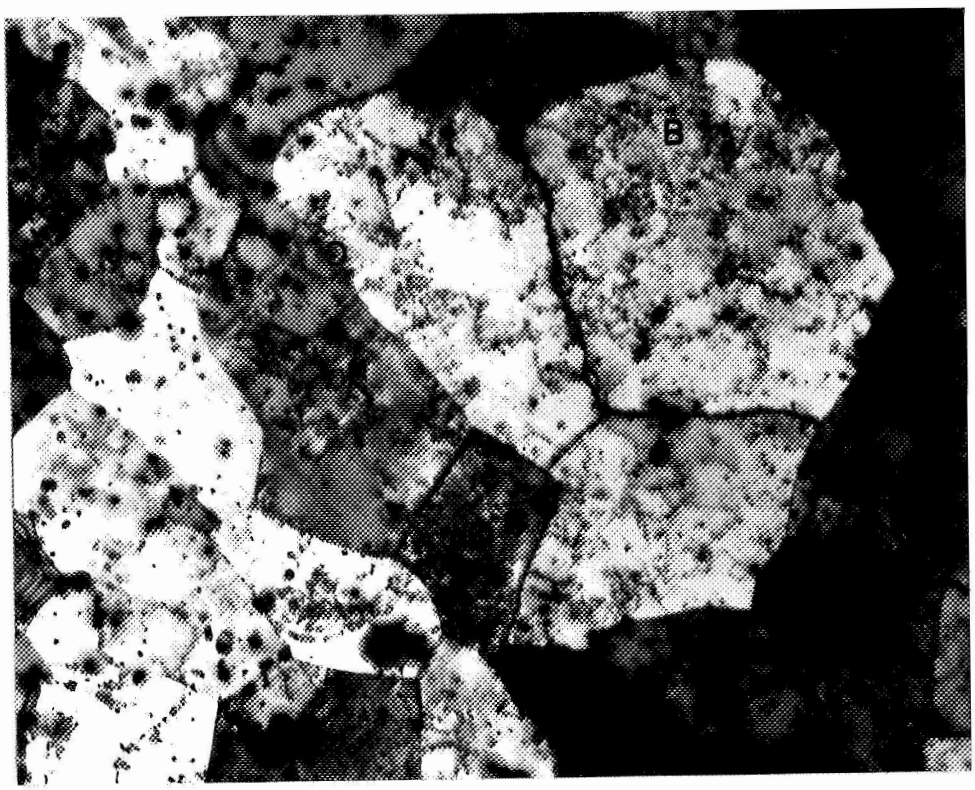

d) Foil normal parallel to bar axis (high magnification). Note dislocations at B, low angle boundary at C, high angle boundary at D.

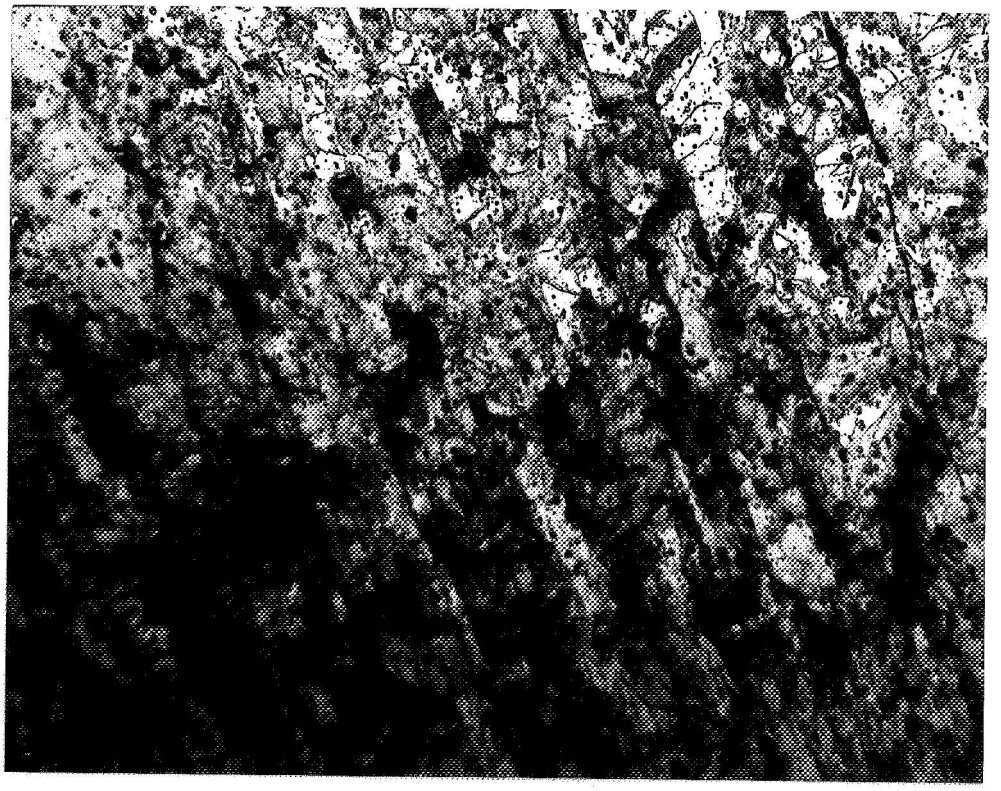

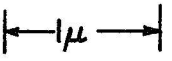

Figure 5. Commercial bar TD-nickel, longitudinal rolling 87% (Foil normal perpendicular to rolling direction).

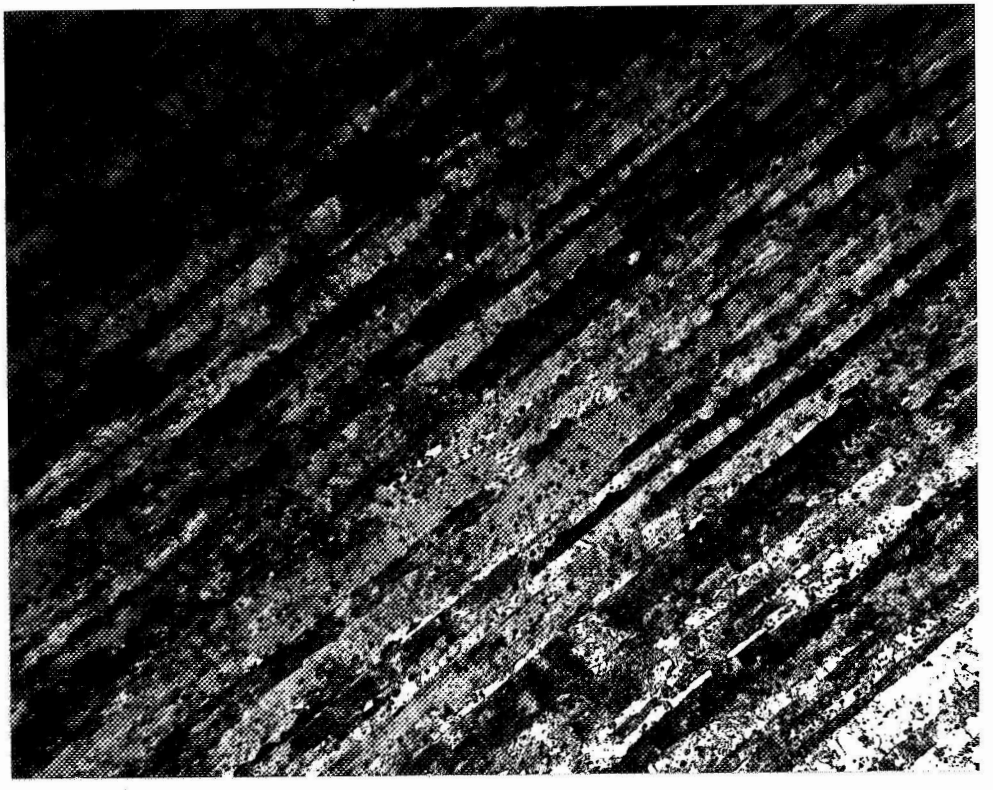

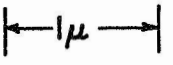

Figure 6. Commercial bar TD-nickel, swaged 90%
(Foil normal perpendicular to swaging direction).

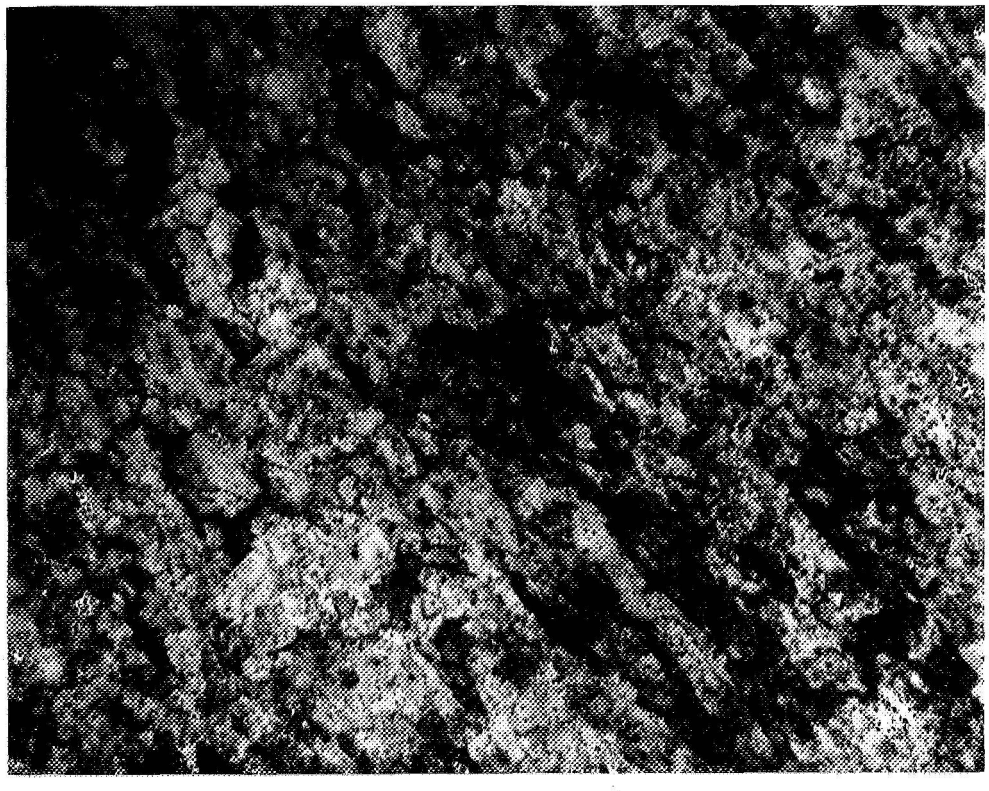

Figure 7. As-extruded TD-nickel, longitudinal rolling 90% (Foil normal perpendicular to rolling direction).

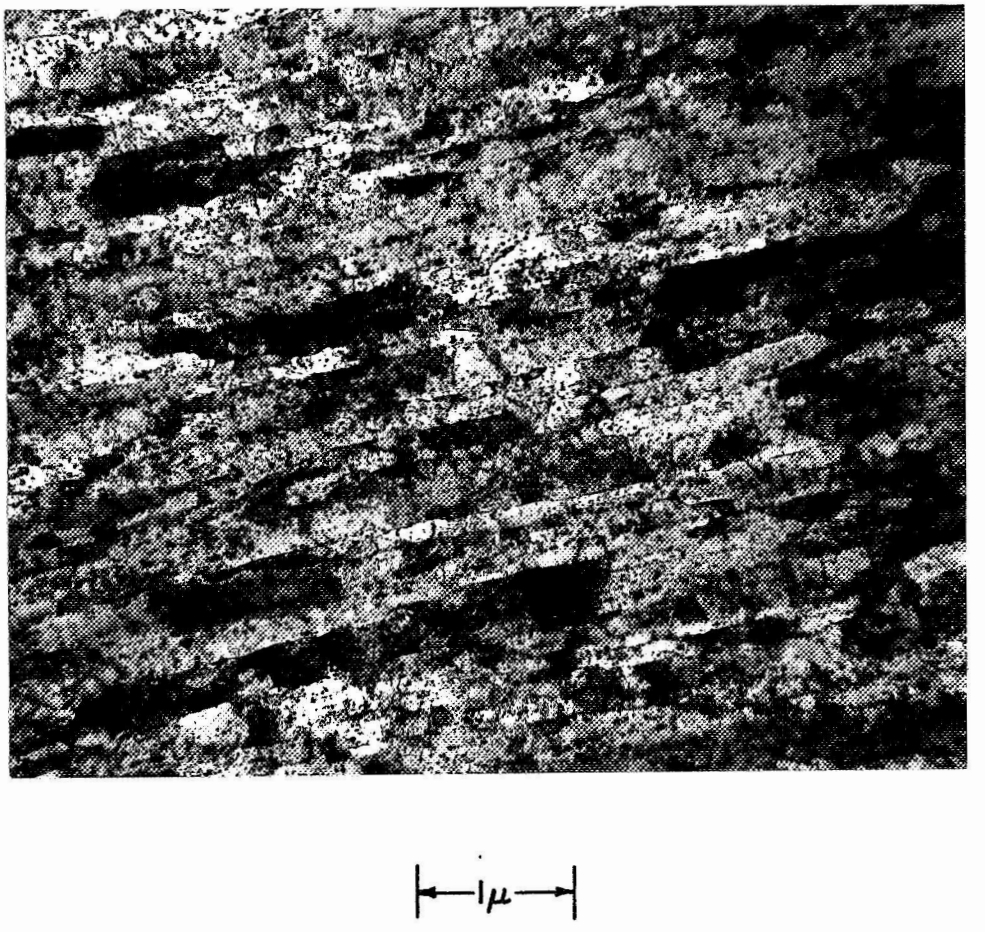

Figure 8. As-extruded TD-nickel, swaged 90%
(Foil normal perpendicular to swaging direction).

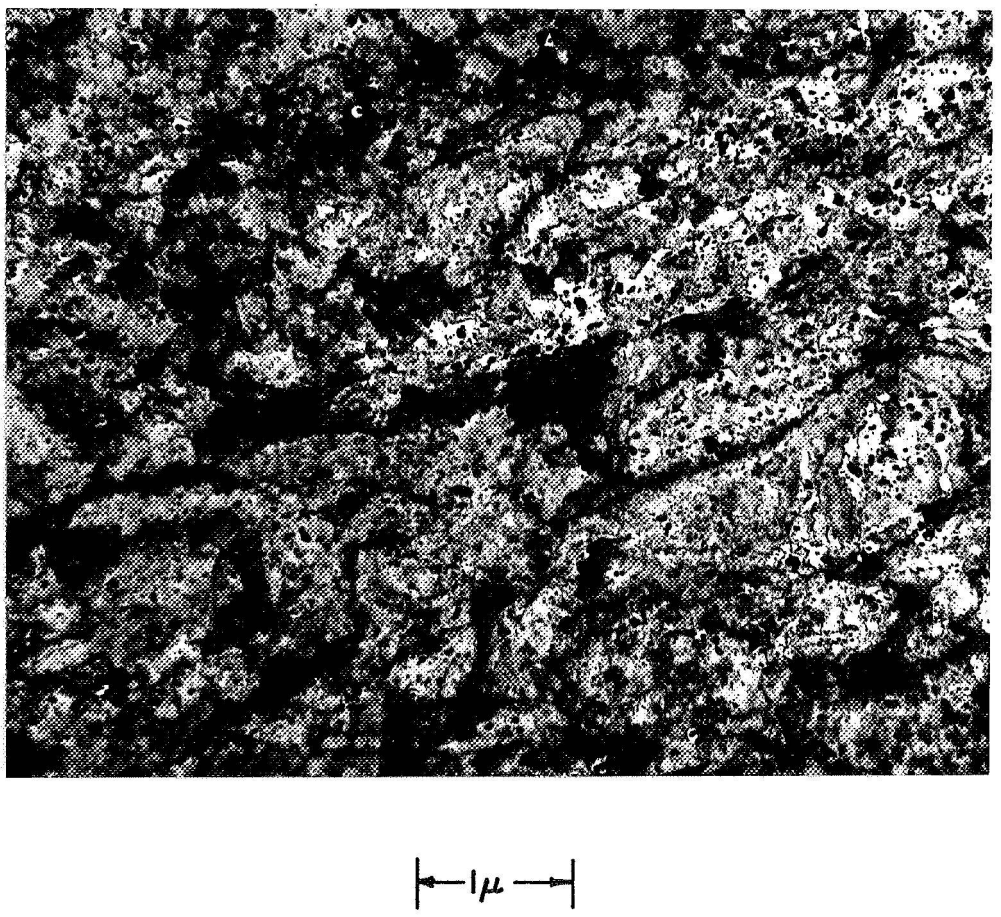

Figure 9. Commercial bar TD-nickel, transverse rolling 83% (Foil normal perpendicular to rolling direction).

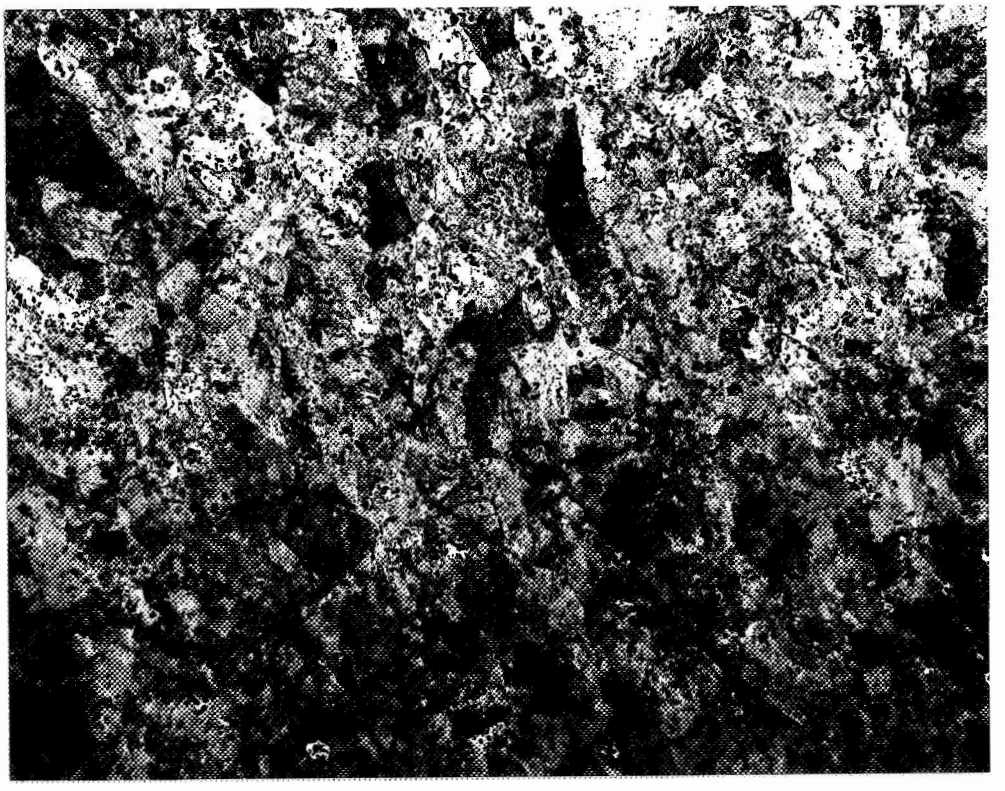

Figure 10. As-extruded TD-nickel, longitudinal rolling 60% (Foil normal perpendicular to rolling direction).

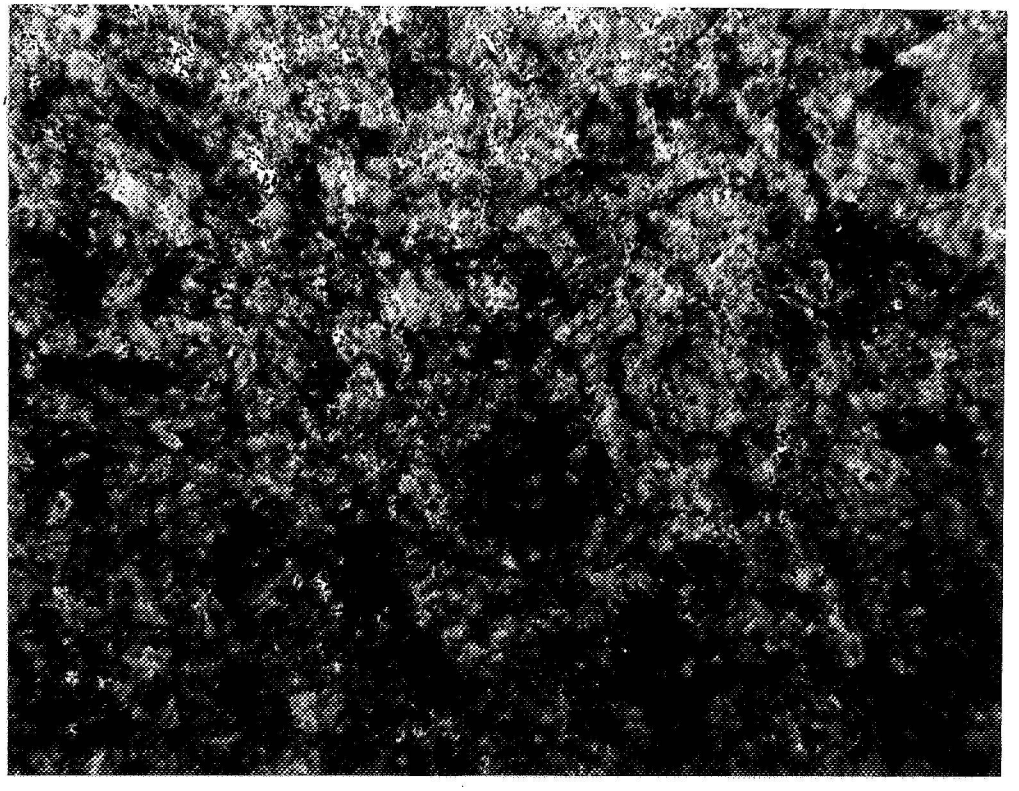

Figure 11. As-extruded TD-nickel, transverse rolling 88% (Foil normal perpendicular to rolling direction).

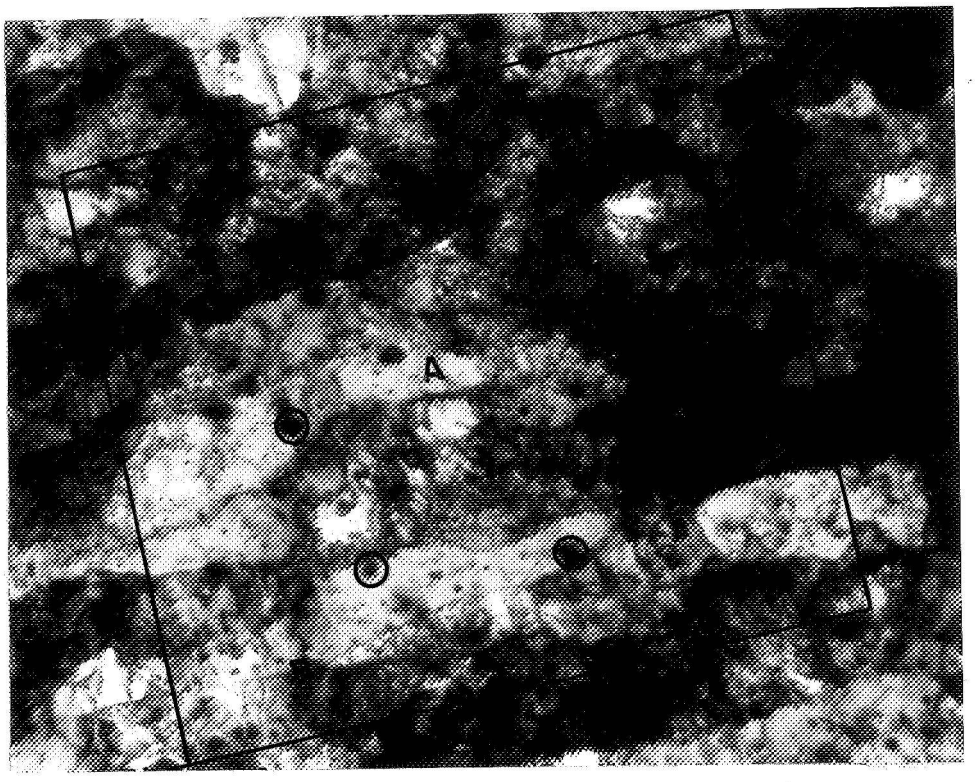

1 μ

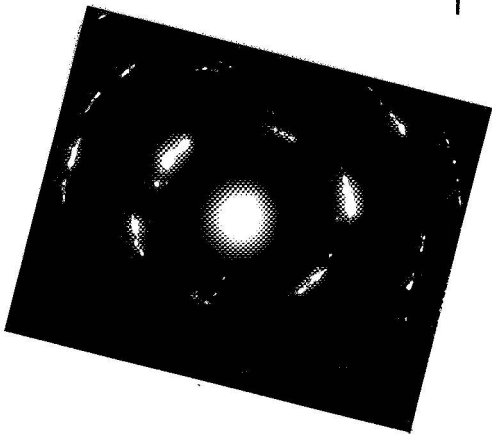

a) 0^{o} Tilt. The area contributing to the diffraction pattern is indicated. Note dislocation cell structure at A, high angle boundary at B. Circled thoria particles are locating points for comparison after tilting.

Figure 12. Commercial bar TD-nickel, longitudinal rolling 87% (Foil normal perpendicular to rolling direction).

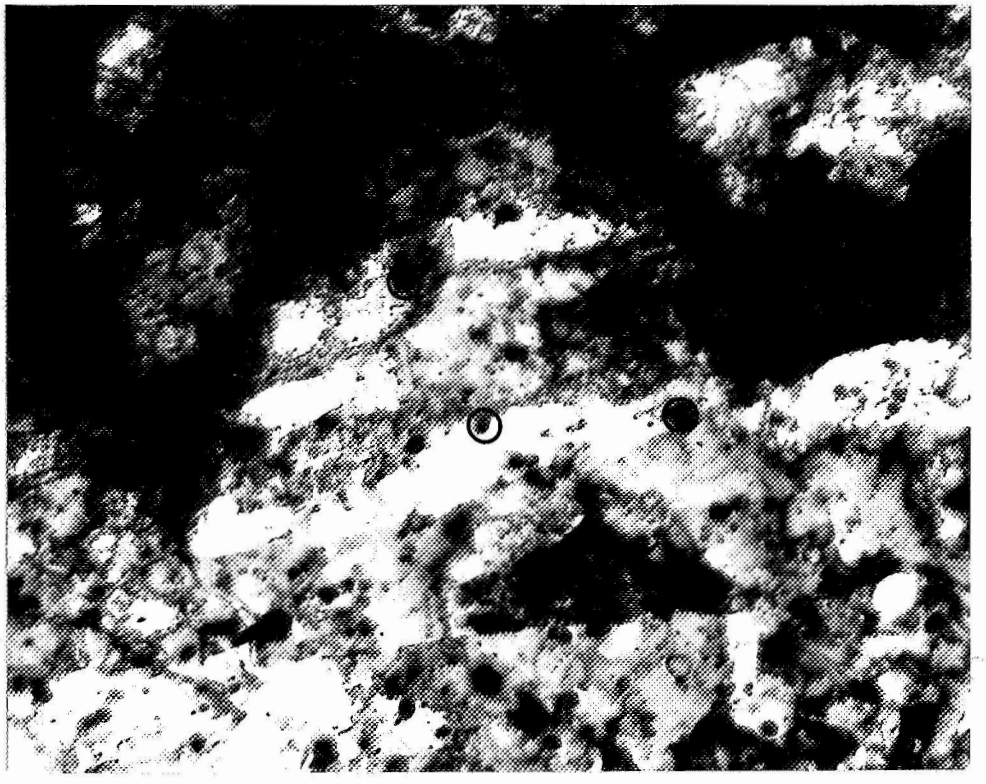

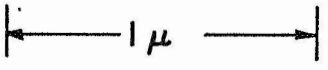

b) 1° Tilt.

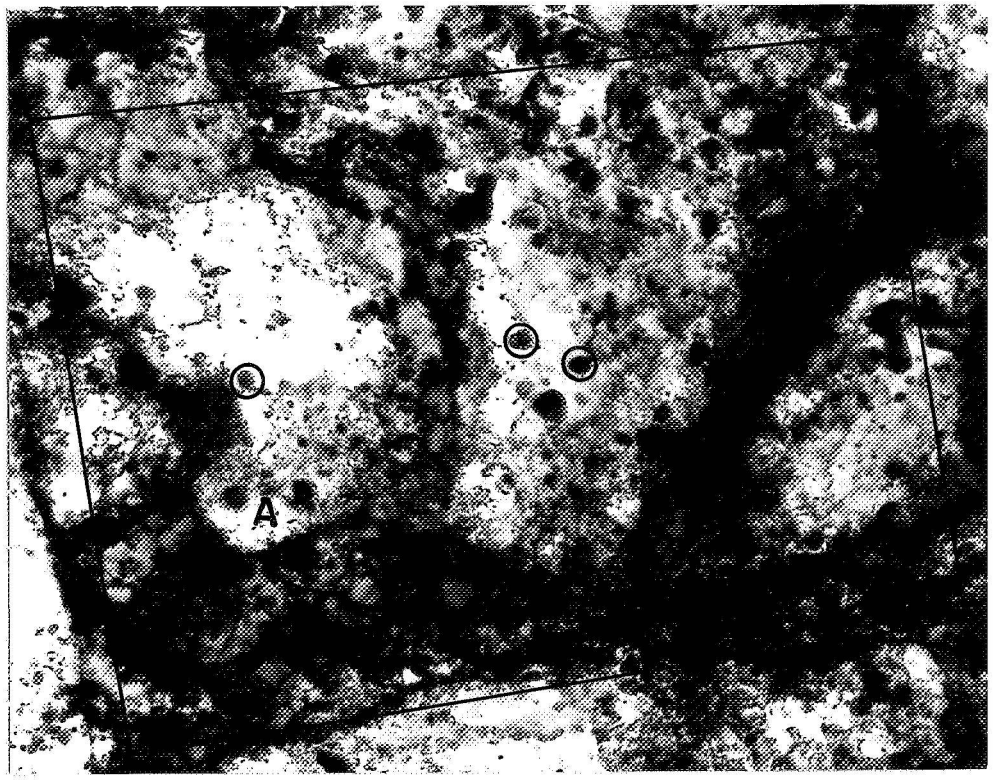

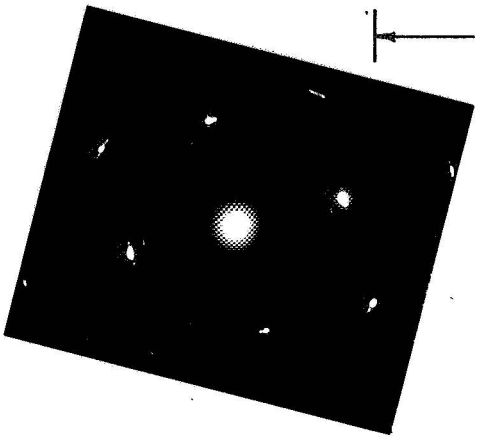

a) 0^{o} Tilt. The area contributing to the diffraction pattern is indicated. Note high dislocation density at A. Circled thoria particles are locating points for comparison after tilting.

Figure 13. Commercial bar TD-nickel, transverse rolling 83% (Foil normal perpendicular to rolling direction).

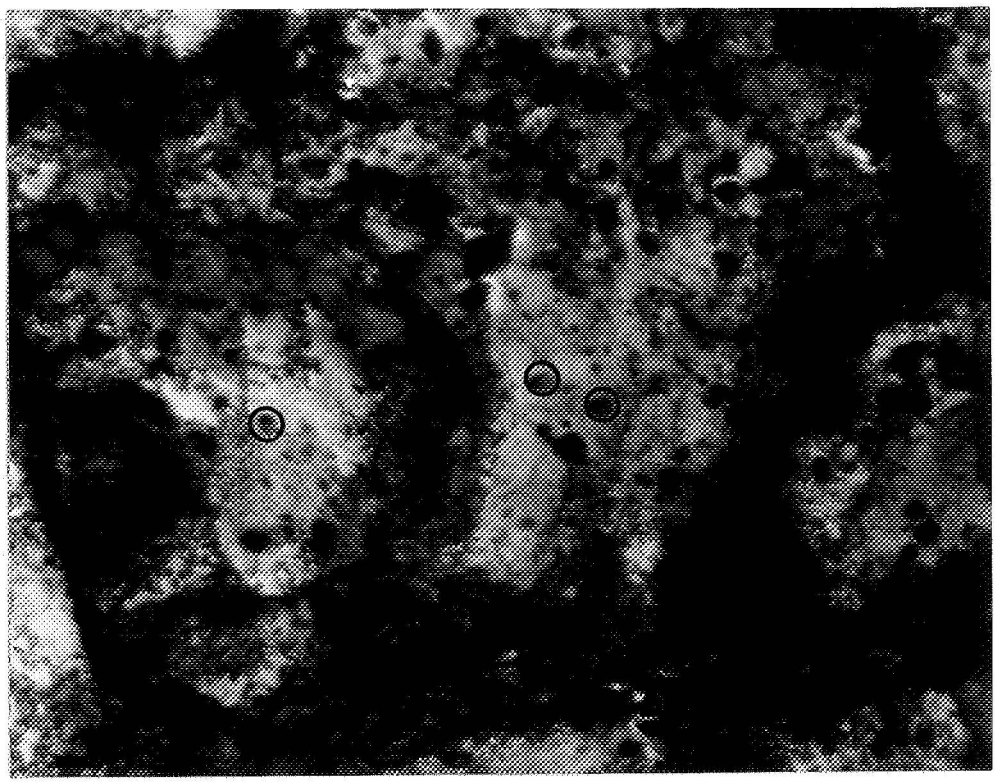

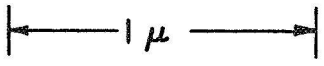

b) 1° Tilt.

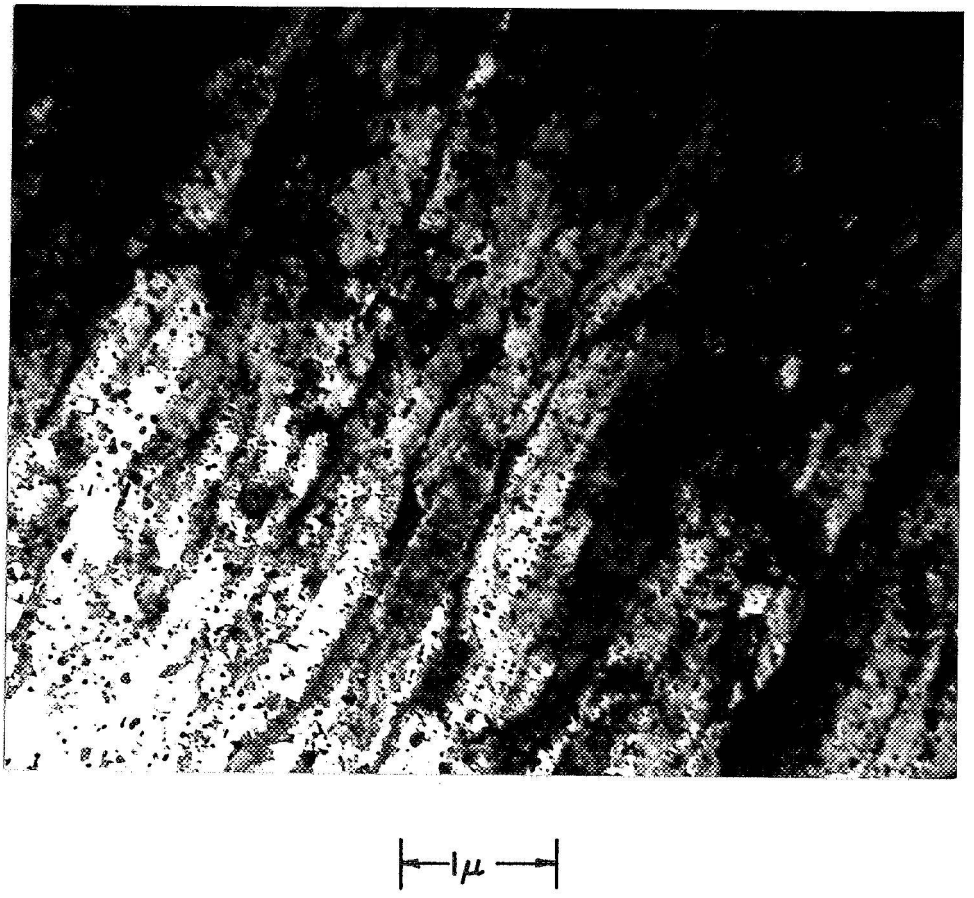

Figure 14. Commercial bar TD-nickel, transverse rolling 24% (Foil normal perpendicular to rolling direction).

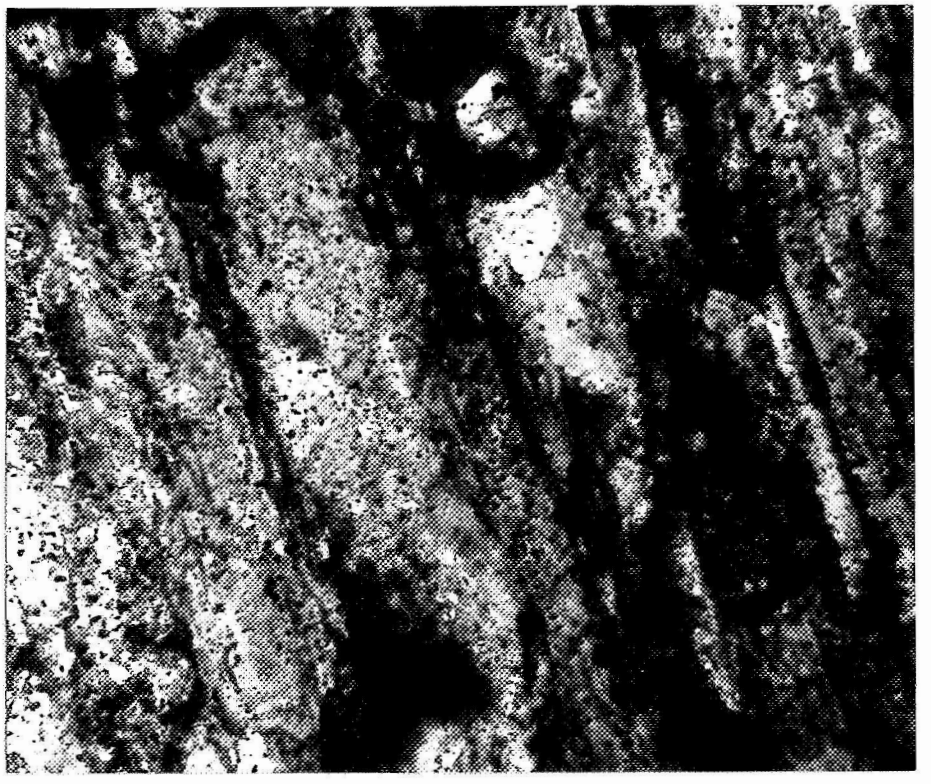

Figure 15. Commercial bar TD-nickel, transverse rolling 37% (Foil normal perpendicular to rolling direction).

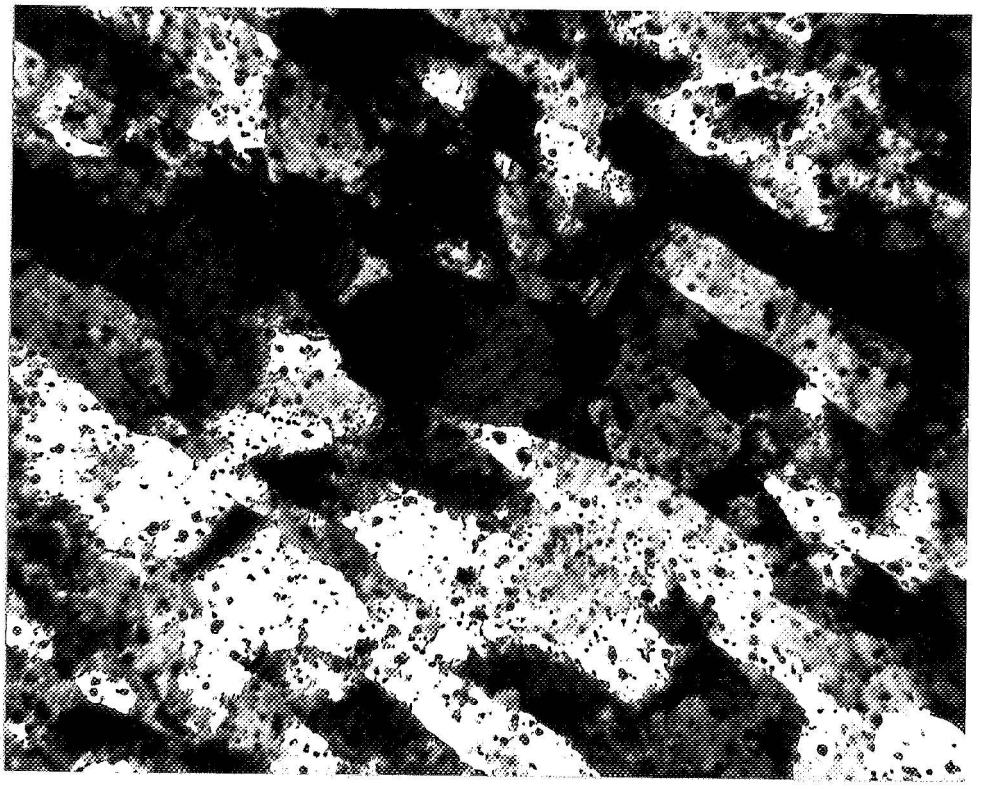

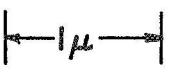

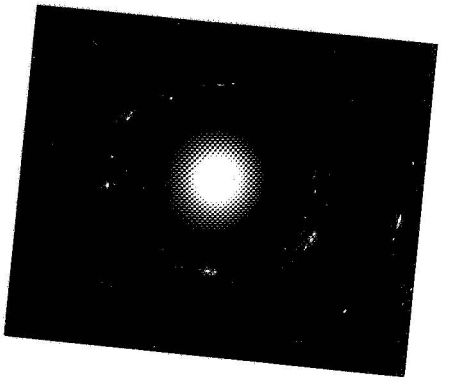

Figure 16. Commercial bar TD-nickel, longitudinal rolling 87%, annealed one hour at 2300°F (Foil normal perpendicular to rolling direction). The entire micrograph area contributed to the diffraction pattern.

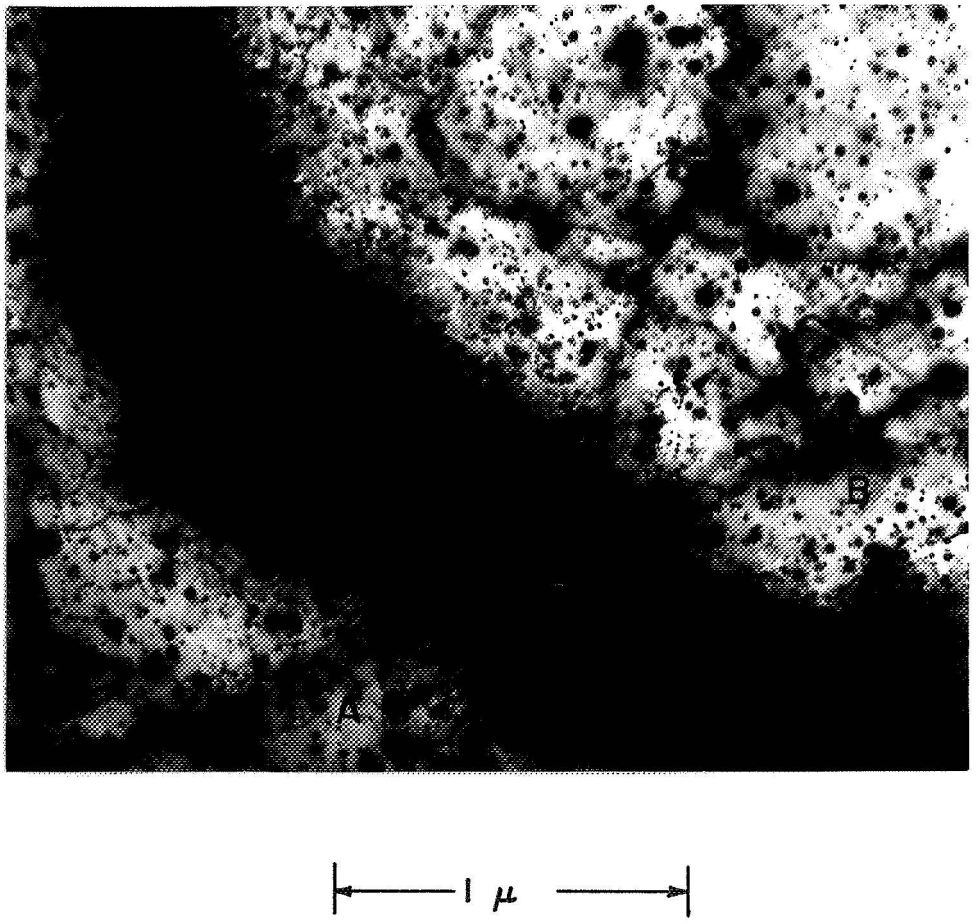

Figure 17. Commercial bar TD-nickel, transverse rolling 87%, annealed one hour at 2300°F (Foil normal perpendicular to rolling direction). Extinction bend contour is a $\underline{G}_{200}$ type. Note low dislocation density at A and B.

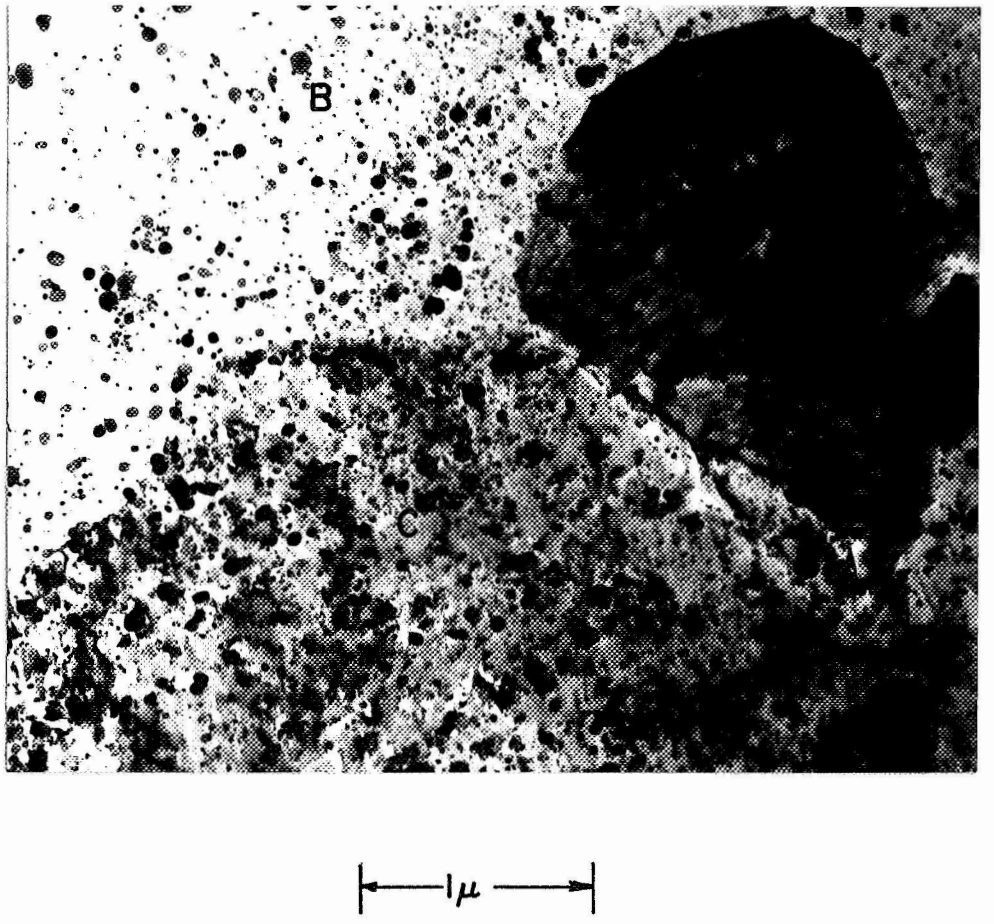

Figure 18. Commercial bar TD-nickel, transverse rolling 87%, annealed one hour at 2300°F (Foil normal perpendicular to rolling direction). Note recovered area at A. Areas B and C are adjacent recrystallized regions.

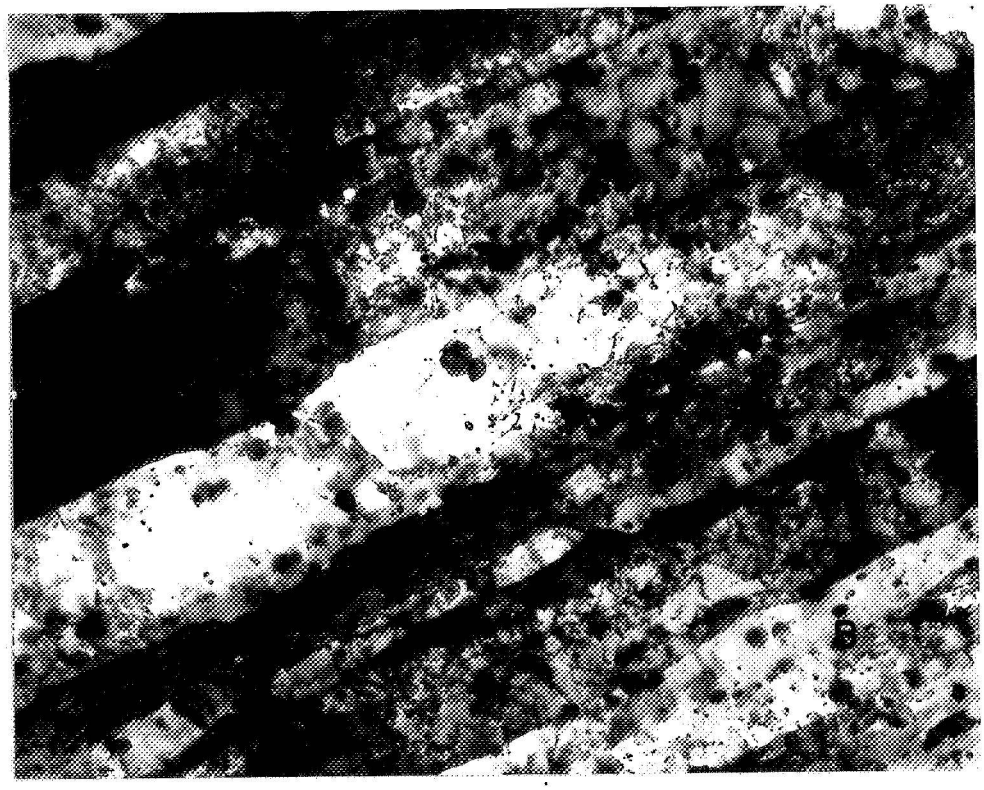

Figure 19. Commercial bar TD-nickel, swaged 90% (Foil normal perpendicular to swaging direction). Thoria particle voids are evident at A and B.